Experimental Investigations of the Turbulent Mixing Process and the Reynolds-Stress Anisotropy Tensor in Ventilated Rooms

Ch. Heschl

Fachhochschulstudiengänge Burgenland GmbH - University of Applied Science, Steinamangerstraße 21, A-7423 Pinkafeld, Austria

W. Sanz

Institute for Thermal Turbomachinery and Machine Dynamics, Graz University of Technology, Inffeldgasse 25, A-8010 Graz, Austria

I. Lindmeier

Fachhochschulstudiengänge Burgenland GmbH - University of Applied Science, Steinamangerstraße 21, A-7423 Pinkafeld, Austria

ABSTRACT

In the past various experimental investigations about room airflows were published. But most investigations are limited regarding measurement positions (restricted flow pattern) and the availability of turbulent quantities (Reynolds-Stresses, entrainment, macroscopic instabilities etc.). Based on the available experimental data a targeted improvement of turbulence models is difficult. Therefore two different room airflow situations were investigated with three-dimensional Particle Image Velocimetry. Detailed information of the flow, the Reynolds-stress distribution and the entrainment are presented. Furthermore stable and nonstable conditions and nonsymmetrical effects are shown. Based on the results the behaviour of RANS-based turbulence models in predicting room airflows is discussed.

1. INTRODUCTION

In the last years the development of ventilation systems was influenced by the demand of energetic efficiency and thermal comfort. To meet the modern requirements validated simulation tools are necessary. Especially the prediction of the standardized thermal comfort parameters PMV (Predicted Mean Vote) and PPD (Predicted Percentage of Dissatisfied) is difficult. In particular the determination of the time-averaged mean velocity and the turbulent intensity distribution is often accompanied by a relatively large uncertainty. In this context the right choice of the turbulence model plays an important role for an accurate CFD modelling - besides the correct simplification of the boundary conditions (e.g. inlet area, inner and outer thermal load etc.). For this reason in the last years many investigations on the accuracy of linear, nonlinear and second moment closure turbulence models were published.

Extensive numerical investigations on two-dimensional room airflows were done in the seventies and eighties (Hanel and Scholz, 1979; Nielsen, 1990 and Kollgaard Voigt, 2000). An important outcome was that isotropic turbulence models (e.g. a linear eddy viscosity model) can accurately predict two-dimensional room airflows.

Due to the availability of powerful workstations since the nineties more complex airflow situations were investigated. Usually, the test airflow was created by a round (nozzle inlet) or plane jet (slot inlet) near the ceiling and the measured data are limited to the jet profile in the median plane of the room (Zhang et al., 2000; Schälin and Nielsen, 2004; Kuznik et al., 2007). Detailed information on three-dimensional effects is only available for standard flow situations such as three-dimensional wall jets (Abrahamsson, 1997). Complete measurement data of the flow pattern in ventilated rooms are not available.

It is generally known that damping of the turbulent fluctuations perpendicular to the wall generates stress-induced axial vorticity (Craft and Launder, 2001). Although the axial vorticity induces a secondary flow (which can substantially influence the flow pattern) the anisotropy tensor distribution in room airflows is not investigated.

So considering the practical relevance of experimental data (validation of turbulence models) further investigations which improve the fundamental understanding of the three dimensional behaviour of complex room airflows are required. In this paper detailed measurement data of the room airflow for two different room geometries are presented. The anisotropy -tensor distribution in the middle of the room is also offered. To avoid an influence of the sensor installations a non-intrusive measurement system is used.

2. Measurement setup

1.1. Test rig

The test rig for the experimental investigations consists of an air supply system with a mass flow meter, a model room made of plexiglass in an air-conditioned test room and a PIV (Particle Image Velocimetry) measurement system. The PIV system is used for two and three dimensional measurements. To record a larger measurement field the two cameras are also used for the two-dimensional measurements. The experimental arrangement is shown in Fig. 1. The test rig is equipped with a frequency-controlled fan unit, which feeds the air via an orifice plate, rectifier, flow measurement unit, temperature sensors and seeding mixing chamber to the plexiglass test model. To get a better illumination the plexiglass model is set inside a black coated test room. In order to minimize the thermal influences the laser energy supply and the computer equipment are placed outside of the test room. To ensure isothermal conditions the test room is additionally ventilated. The inlet air temperature, the outlet air temperature and the surface temperature of the surrounding walls of the plexiglass model are continuously monitored by 10 Pt100 temperature sensors. Also the ambient pressure and the inlet mass flow are monitored. The light sheet optic and the two cameras are mounted on a two dimensional traverse system, so that only one calibration for the PIV measurements has to be done.

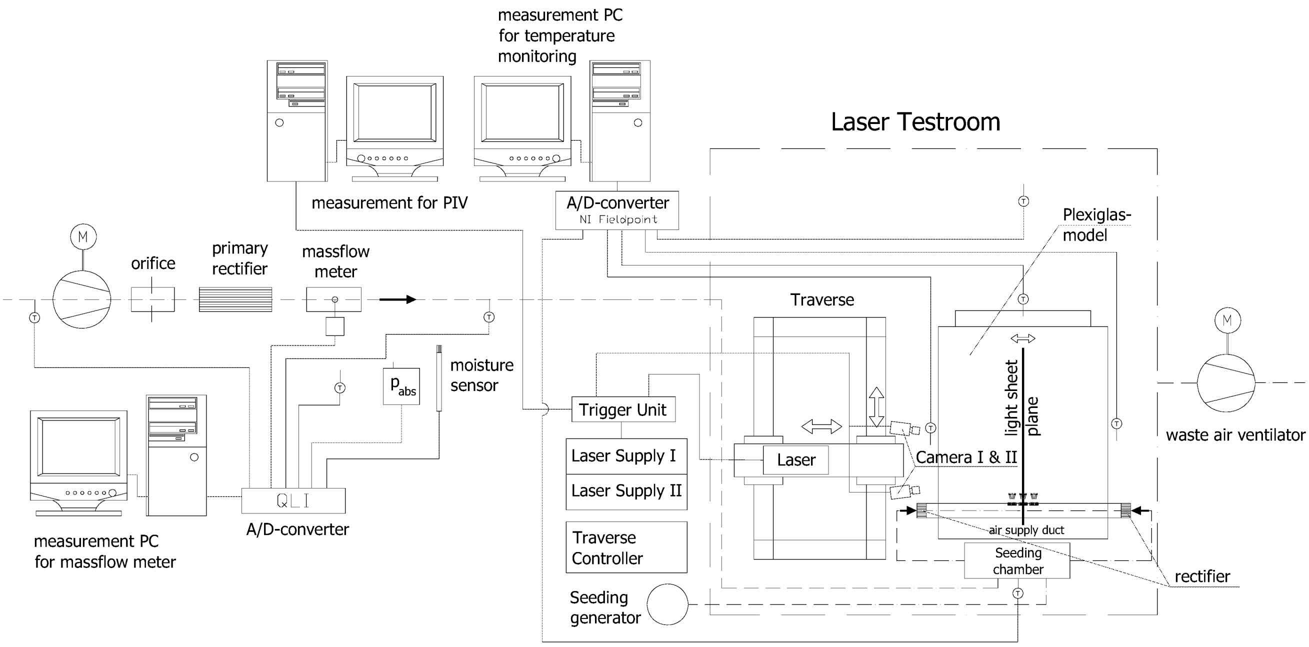

Figure 1. PC for temperature monitoring, PIV PC, PC for massflow meter, exhaust air fan

During the measurement the temperatures, the relative humidity and the ambient pressure are logged, so that the air properties can be determined.

The measurement planes are chosen in such a way that the whole flow area in the x-y plane can be measured by moving the lightsheet and camera with the traverse system.

1.2. Plexiglass models

The dimensions of the plexiglass models are shown in Figs. 2 and 3.

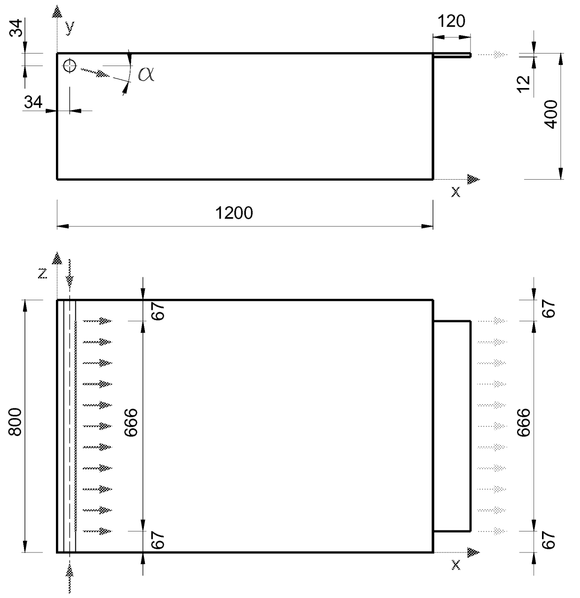

Figure 2. Geometry of the plexiglass model room I (dimensions in mm)

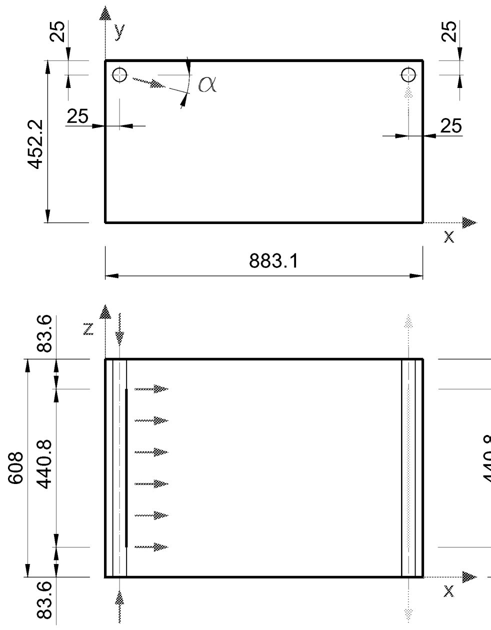

Figure 3. Geometry of the plexiglass model room II (dimensions in mm)

The plexiglass models differ by different length-to-height and length-to-width ratios and by different outlet openings. Both models have an air supply duct (38 x 3mm) with evenly distributed holes. Both supply ducts are fed from both end sides over a flow rectifier.
The air supply duct of the first model has 222 holes with a diameter of 2 mm and a distance between the holes of 3 mm. The overall inlet and outlet length is 666 mm. The mean inlet velocity is 14.84 m/s and the inlet angle is 16° measured to the horizontal direction. The air leaves the model through a small channel at the opposite side.
The air supply duct for the second model has 7 groups of 32 holes with a diameter of 1.3 mm and an overall length of 440.8 mm. The distance between the holes is 1.5 mm and between the seven-hole groups 13.5 mm. The mean inlet velocity is 36.88 m/s and the inlet angle is 27.5° measured to the horizontal direction. The outlet is also defined by a duct which has the same hole distribution as the air supply duct - but the holes are aligned below.
For the second model the arrangement of the supply holes is shown in detail in Fig. 4.

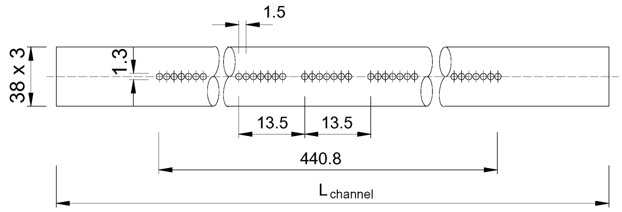

Figure 4. Principle geometry of the air supply duct for the plexiglass model room II

All measurements are done at isothermal boundary conditions.

1.3. PIV measurement setup

Three different measurement campaigns were performed. The first and third measurement campaigns serve to acquire the mean flow pattern in the model room I and II. Because of the large number of measuring points a two dimensional PIV setup is used. The second measurement is performed in order to determine the turbulent stresses in the mid plane of model room I. For this test three-dimensional PIV measurements of a large number of samples were taken. For all PIV measurements two cameras with a resolution of 1344 x 1024 pixels are used. The interrogation areas are defined with 32x32 pixels and an overlapping of 25%. For the determination of the velocity vectors the adaptive correlation method (Dantec, 2002) is used. In z-direction the velocity distribution were measured by traversing the lightsheet and cameras in steps of 20 mm for the 2D and 10 mm for the 3D measurements. The details of the three different measurement setups are described in the next sections.

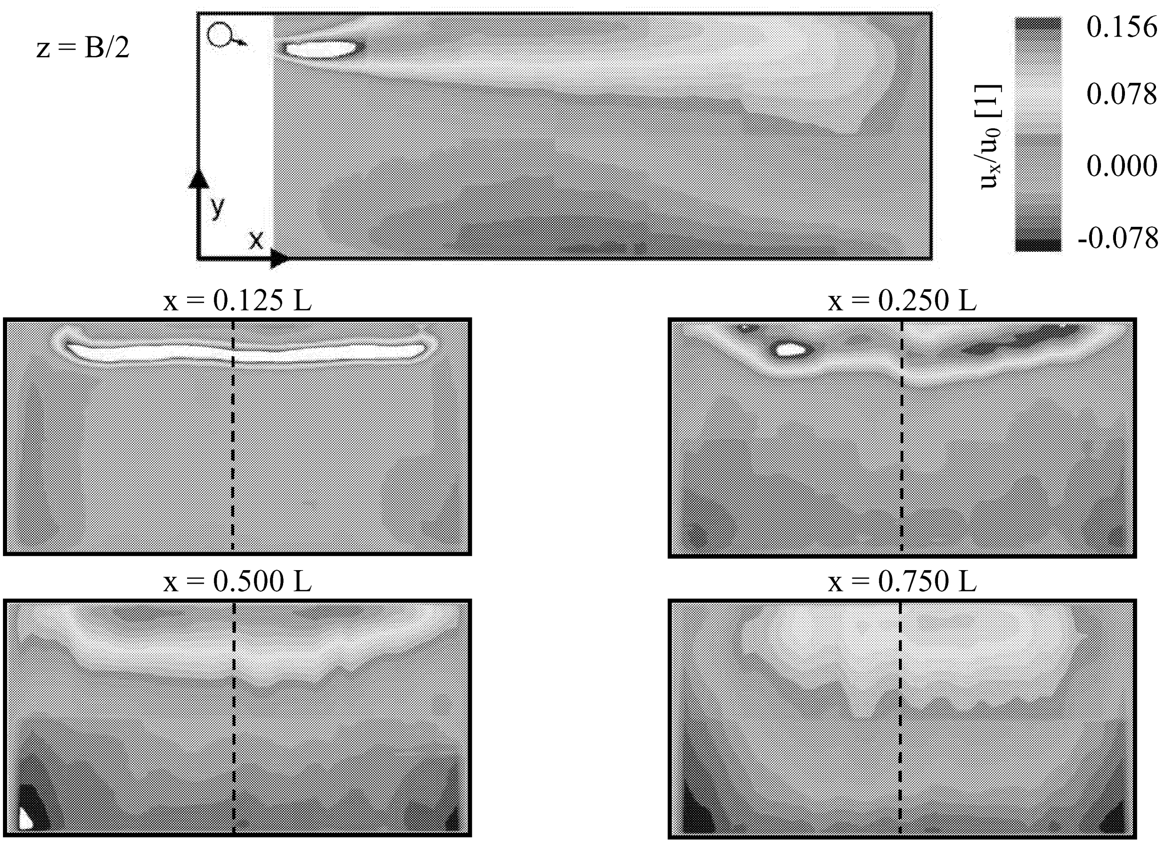

Figure 5. Measured dimensionless x-velocity component for the model room I at z=B/2 and at different x positions (the dashed line ----- corresponds to z=B/2).

1.3.1. 2D PIV setup for the plexiglass model I

The two cameras are mounted on top of each other so that the complete height of the model room can be covered. The field of view of one camera is 155 x 200 mm², so that in x-direction 294, in y-direction 110 and in z-directions 39 measured positions were obtained. This yields in a measured domain x = 110 to 1.200mm, y = 0 to 400mm and z = 0 to 800mm which consists of about 1.300.000 vectors. In order to eliminate the turbulent fluctuations the measuring data are averaged over a measuring period of 30 seconds with a sample rate of 4 Hz.

1.3.2. 3D PIV setup for the plexiglass model I

For this measurement the two cameras are mounted in an angle of 70° and 130°, respectively, to the x-axis of the plexiglass model. The field of view of the cameras is 84 x 110 mm². The measurement plane is located in the mid of the room (x=600mm). In z-direction data are collected in steps of 10 mm from z = 0 to z=B/2 (B corresponds to the room width). The measurement period is 300 seconds with a sample rate of 2 Hz.

1.3.3. 2D PIV setup plexiglass model II

In this case also two cameras are mounted on top of each other but the field of view of one camera is only 73 x 98 mm² so that the complete height of the model room couldn't be measured. The measurement period is 300 seconds with a sample rate of 2 Hz.

2. Measurement results

The Figs. 5 and 6 show the distribution of the dimensionless x-velocity component (u_0 is the averaged inlet velocity) at z=B/2 and at different x planes of the investigated plexiglass models. In both cases a free jet develops after the inlet. The ambient air is entrained by the turbulent mixing process so that the single jets merge to a

plane jet. Because of the ceiling too little air can be entrained from above. Therefore an underpressure arises that presses the jet towards the ceiling (Coanda effect) so that a three dimensional wall jet – which is reflected by the back wall - developes. Consequently there is an interaction between the wall jet on the ceiling and the reflected air flow (illustrated by the positive and negative x-velocity distribution in the Figs. 5 and 6).
In addition the figures indicate that due to the gap between the inlet area and the side walls an entrainment of air occurs which induces a cross flow. This makes the jet flow strongly three dimensional. The velocity distribution in the x-planes shows that the flow in the first room is nearly symmetrical to the mid plane and in the second room asymmetrical. During the measurement the position of the jet centre line didn't change so that the asymmetric flow is a stable flow condition. Which side the jet attaches to depends on the starting process (initial-value problem) and is of stochastic nature. This was observed in additional long time measurements with different initial flow conditions.

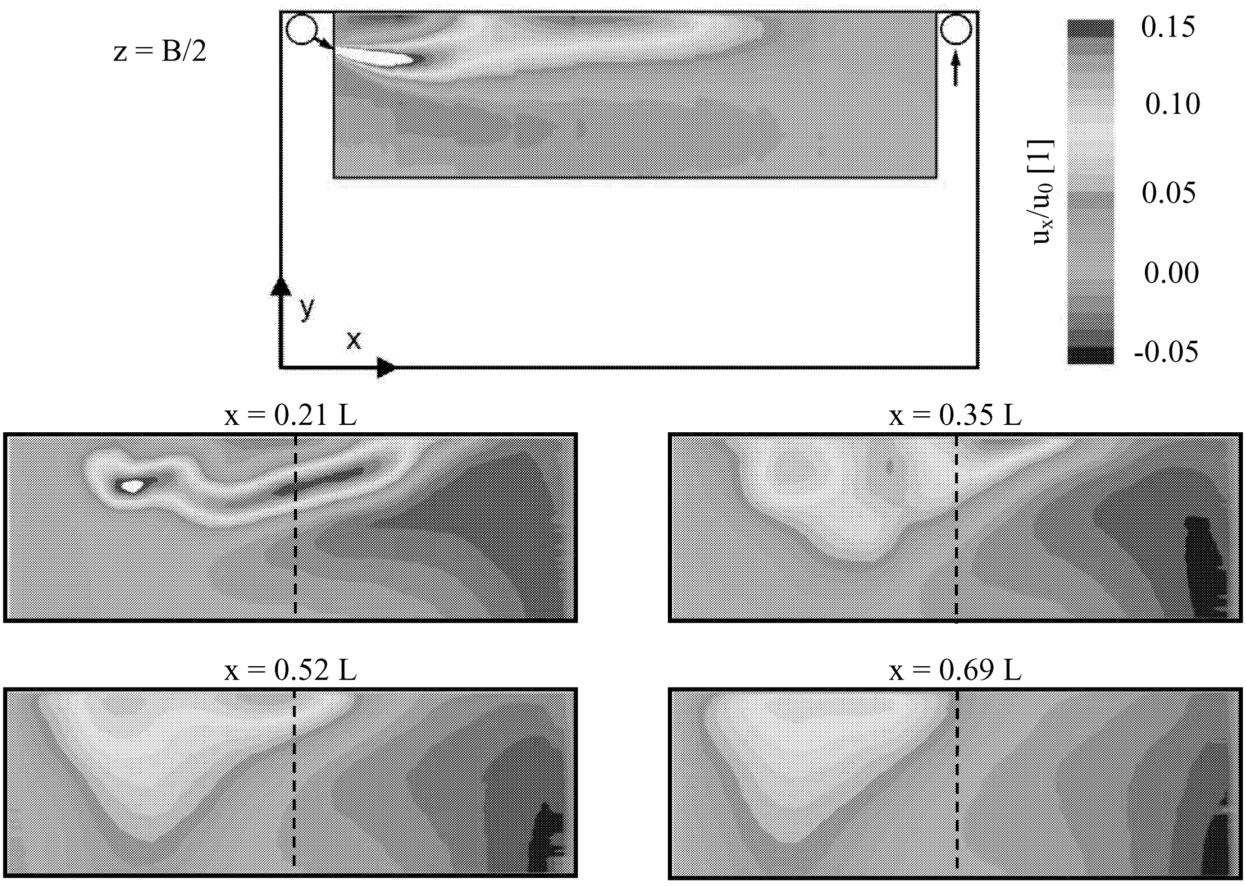

Figure 6. Measured dimensionless x-velocity component for the model room II at z=B/2 and at different x positions (the dashed line ----- corresponds to z=B/2).

Looking at the development of the jet in x-direction it can be seen that in the first model room the jet contraction is clearly smaller as in the second one. Compared with free-shear flows the contraction rate of the wall jet in model room I is clearly bigger. Thus additional forces which contract the wall jet in the z-direction must be present.
After about x=L/3 the jet is fully attached to the ceiling so that the under pressure between the jet and the ceiling can be neglected as force. Another potential force can be derived from the local changes of the difference between lateral and perpendicular-to-the-ceiling turbulent normal stresses. Well-known effects of this kind due to the turbulent anisotropy are Prandtl's second type of secondary motion and the

remarkable spreading behavior of three-dimensional wall jets (Abrahamsson, 1997; Craft and Launder, 2001).

In order to investigate the influence of the Reynolds stresses on the secondary flow the anisotropy tensor b_{ij} is determined from the three-dimensional PIV measurements (see section 1.3.2). Since the difference between the lateral and perpendicular-to-the-wall normal stresses produces a vorticity vector inducing the secondary motion, only the difference of the components b_{33} and b_{22} is investigated. For the plane x=L/2 (x=600mm) the difference of the anisotropy tensor is shown in Fig. 7.

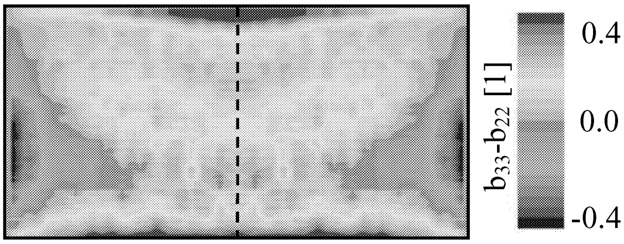

Figure 7. Measured difference of the anisotropy tensor b_{33}-b_{22} in the x=600mm plane for the model room I (the dashed line ----- correspond to z=B/2 and the mirror plane respectively).

The $b_{33} - b_{22}$ distribution indicates that near all walls the perpendicular component of the turbulent normal stress strongly increases similar to the situation observed by three-dimensional wall jets or rectangular ducts. In both cases only a second moment closure model (Reynolds stress turbulence model) is able to reproduce the flow behaviour. Therefore it can be concluded that an accurate prediction of wall-affected room airflows requires a higher order turbulence model which is able to reproduce the turbulent normal stress distribution.

3. Summary and Conclusion

In this paper 2D and 3D PIV measurement results of the flow and the turbulence quantities in ventilated rooms are presented. Although exact symmetrical boundary conditions are used asymmetrical room airflows can also be observed. Furthermore, for wall bounded flows strong Reynolds stress anisotropy near the ceiling, floor and side walls can be detected. It can be concluded that in such cases an accurate prediction of the room airflow needs more sophisticated turbulence model (second moment closure).

Nomenclature

k .... kinetic turbulence energy [m²/s²]

b_{ij} .... Reynoldsstress anisotropy tensor [1]

$$b_{ij} = \left(\overline{u'_i u'_j} - 2/3\,k\delta_{ij}\right)/\,2k$$

$\overline{u'_i u'_j}$ ... Reynoldsstress tensor [m²/s²]

References

Abrahamsson, H. (1997): On Turbulent Wall Jets. PhD thesis, Department of Thermo and Fluid Dynamics, Chalmers University of Technology: Göteburg Sweden. ISBN 91-7197-491-1

Craft T.J., Launder B.E. (2001): On the spreading mechanism of the three-dimensional turbulent wall jet. Journal of Fluid Mechanics, Vol. 435: Pages 305-326.

Dantec (2002). FlowManager software and Introduction to PIV Instrumentation. Software User's guide. Dantec Dynamics Publication No. 9040U3625.

Hanel, B., Scholz, R. (1979). Beitrag zur Modellierung zweidimensionaler isothermer und nichtisothermer turbulenter Strömungen in Räumen – Teil I. Luft- und Kältetechnik, 3: Pages 154 – 157.

Kollgaard Voigt, L.P. (2000). Comparison of Turbulence Models for Numerical Calculation of Airflow in an Annex 20 Room. International Centre for Indoor Environment and Energy, Department of EnergyEngineering, Technical University of Denmark, ISBN 87-7475-225-1.

Kuznik, F., Rusaouen, G. and Brau, J. (2007). Use of a RSM Turbulence Model for the Prediction of Velocity and Temperature Fields in a Mechanically Ventilated Room. International Journal of Ventilation ISSN 1473-3315 Volume 6 No 2

Nielsen, P.V. (1990). Specification of a Two-dimensional Test Case, International Energy Agency, Annex 20: Air Flow Pattern Within Buildings., Department of Building Technology and Stuctural Engineering, Aborg University, ISSN 09902-7513 R9040: Pages 11-15

Schälin, A., Nielsen, P.V. (2004): Impact of turbulence anisotropy near walls in room airflow. Indoor Air 2004, Vol. 14: Pages 159-168.

Zhang, G., Morsing, S., Bjerg, B. und Svidt, K. (2000). A Study on the characteristics of airflow in a full scale room with a slot wall inlet beneath the ceiling. Proceedings if RoomVent'2000: Pages 199-204.